A Kinetic and Mechanistic Study of the Reactions of OH Radicals and Cl Atoms with 3,3,3-Trifluoropropanol under Atmospheric Conditions

Tanya Kelly,[†] **Valérie Bossoutrot,**[‡] **Isabelle Magneron,**[‡] **Klaus Wirtz,**[§] **Jack Treacy,**[†]
Abdelwahid Mellouki,[‡] **Howard Sidebottom,***[,†] **and Georges Le Bras**[‡]

Chemistry Department, University College Dublin, Belfield, Dublin 4, Ireland, Laboratoire de Combustion et Systèmes Réactifs, Centre Nationale de la Recherche Scientifique, Orléans, France, and Fundación Centro de Estudios Ambientales del Mediterráneo, Parque Tecnológico de Paterna Valencia, Spain

Received: July 22, 2004; In Final Form: November 1, 2004

Product distribution studies of the OH radical and Cl atom initiated oxidation of $CF_3CH_2CH_2OH$ in air at 1 atm and 298 ± 5 K have been carried out in laboratory and outdoor atmospheric simulation chambers in the presence and absence of NO_x. The results show that CF_3CH_2CHO is the only primary product and that the aldehyde is fairly rapidly removed from the system. In the absence of NO_x the major degradation product of CF_3CH_2CHO is CF_3CHO, and the combined yields of the two aldehydes formed from $CF_3CH_2CH_2OH$ are close to unity (0.95 ± 0.05). In the presence of NO_x small amounts of $CF_3CH_2C(O)O_2NO_2$ were also observed (<15%). At longer reaction times CF_3CHO is removed from the system to give mainly CF_2O. The laser photolysis−laser induced fluorescence technique was used to determine values of $k(OH + CF_3CH_2CH_2OH) = (0.89 \pm 0.03) \times 10^{-12}$ and $k(OH + CF_3CH_2CHO) = (2.96 \pm 0.04) \times 10^{-12}$ cm^3 molecule^{-1} s^{-1}. A relative rate method has been employed to measure the rate coefficients $k(OH + CF_3CH_2CH_2OH) = (1.08 \pm 0.05) \times 10^{-12}$, $k(OH + C_6F_{13}CH_2CH_2OH) = (0.79 \pm 0.08) \times 10^{-12}$, $k(Cl + CF_3CH_2CH_2OH) = (22.4 \pm 0.4) \times 10^{-12}$, and $k(Cl + CF_3CH_2CHO) = (25.7 \pm 0.4) \times 10^{-12}$ cm^3 molecule^{-1} s^{-1}. The results from this investigation are discussed in terms of the possible importance of emissions of fluorinated alcohols as a source of fluorinated carboxylic acids in the environment.

Introduction

The phase out of chlorofluorocarbons (CFCs) due to their implication in stratospheric ozone depletion has been well documented[1,2] and a number of hydrofluorocarbons (HFCs) and hydrochlorofluorocarbons (HCFCs) have been developed as replacement compounds. These compounds are susceptible to attack by OH radicals and therefore can be oxidized in the troposphere.[3] In general, HFCs and HCFCs have rather long atmospheric lifetimes and have large global warming potentials.[3] Partially fluorinated alcohols have been suggested as alternatives to CFCs in applications such as the cleaning of electronic components, refrigeration, and carrier compounds for lubricants. Long-chain (C_8−C_{12}) perfluoro alcohols have been detected in the atmosphere and it has been suggested that oxidation of these compounds could provide a source of the perfluorocarboxylic acids found in the environment.[4,5] Although perfluoro alcohols have few direct uses they are employed extensively in the manufacture of fluorinated polymeric materials into which they are incorporated through the OH group. It has been speculated that the eventual degradation of the polymers releases the alcohols into the troposphere.[4,5] A number of experimental studies have been reported on the kinetics and mechanisms for the oxidation of fluoro alcohols.[4,6−10] The available evidence suggests that fluoro alcohols are considerably less reactive than the parent alcohols and that the major oxidation products are the corresponding aldehydes.[5,9−11] In this work kinetic and product distribution studies for the reactions of OH radicals and Cl atoms with 3,3,3-trifluoropropanol were carried out in laboratory reaction chambers and at the European outdoor simulation chamber (EUPHORE) at Valencia, Spain. In addition, the rate coefficient for the reaction of OH radicals with 3,3,4,4,5,5,6,6,7,7,8,8,8-tridecafluorooctanol was determined. The results are used to assess the likely environmental impact of releases of fluid fluoro alcohols into the troposphere.

Experimental Section

Relative Rate Studies. Reactions were carried out at 298 ± 2 K and atmospheric pressure in two different collapsible FEP Teflon reaction chambers, with volumes of approximately 50 and 150 L each. The temperature of the reaction chambers was thermostatically controlled and electric fans positioned below each chamber helped maintain a constant temperature. The reaction chambers were surrounded by banks of fluorescent lamps, which provided sources of radiation at 254 nm (Philips germicidal lamps TUV, 15W) and in the 300−450 nm wavelength region with a maximum intensity around 358 nm (Philips black lamps TL 20/08). The reaction chambers were approximately half-filled by a diluent gas, typically zero-grade air, via Teflon tubing, using calibrated flow meters. Measured pressures (MKS Baratron capacitance manometers) of the reactants were then expanded into the evacuated vacuum line and isolated in a calibrated mixing bulb, from which they were swept into the reaction chamber by a stream of zero-grade air. Tridecafluorooctanol, which has a very low vapor pressure, could not be introduced into the chamber in this manner. A

---

* To whom correspondence should be addressed. Phone: +353-(0)1-7162293. Fax: +353-(0)1-7162127.

[†] University College Dublin.

[‡] Centre Nationale de la Recherche Scientifique.

[§] Fundación Centro de Estudios Ambientales del Mediterráneo.

10.1021/jp0467402 CCC: $30.25

measured volume of a liquid sample was deposited on sintered glass and flushed into the chamber by purified air. Hydrogen peroxide solution and water (triply distilled) were both injected directly into the chamber. Ozone was generated by passing zero-grade air through an ozone generator (Monitor Labs) and the ozone produced was flowed into the reaction chamber. When all the reactants had been added to the chamber it was subsequently filled to capacity at ca. 1 atm of pressure and kept in the dark for 1 h to allow complete mixing of the reactants. A homogeneous reaction mixture was confirmed by consistent, reproducible gas chromatographic analysis.

Hydroxyl radicals were generated by the photolysis of hydrogen peroxide:

$$H_2O_2 + h\nu\ (\lambda = 254\ \text{nm}) \rightarrow OH + OH \qquad (1)$$

or by the photolysis of ozone at 254 nm in the presence of water vapor:

$$O_3 + h\nu\ (\lambda = 254\ \text{nm}) \rightarrow O(^1D) + O_2 \qquad (2)$$

$$O(^1D) + H_2O \rightarrow OH + OH \qquad (3)$$

Molecular chlorine was photolyzed to produce chlorine atoms:

$$Cl_2 + h\nu\ (\lambda > 300\ \text{nm}) \rightarrow Cl + Cl \qquad (4)$$

Typical initial mixing ratios employed were $[\text{substrate}]_0 = [\text{reference}]_0 = 15-80$ ppm; $[O_3]_0 = \sim 50$ ppm, $[H_2O]_0 \approx 2000$ ppm, and $[H_2O_2]_0 = 500$ ppm. For the chlorine atom initiated reactions, photolyses of substrate, reference, and Cl_2 mixtures were carried out with $[\text{substrate}]_0 = [\text{reference}]_0 = 20-70$ ppm and $[Cl_2]_0 = 40-120$ ppm. Mixtures of substrate, reference, and radical precursors were photolyzed until about 50% depletion of the substrate or reference compound had occurred. These conversion levels minimize any complications arising from secondary chemistry and competing reactions of primary photolysis products. Quantitative analyses of the relative rate experimental reaction mixtures were achieved by gas chromatography (Shimadzu GC 8A or Varian 3600) coupled with flame ionization detection and Fourier transform infrared spectroscopy (FTIR). A Mattson Galaxy 5000 or a Nicolet Magna 550 FTIR, fitted with mercury cadmium telluride (MCT) detectors, was used for the infrared analyses of reaction mixtures. Each spectrometer was fitted with an evacuable 2 L Teflon-coated Wilks cell, containing a multipass White mirror arrangement (10 m path length), to facilitate the collection of infrared spectra. Spectra were recorded over the range $400-4000\ \text{cm}^{-1}$ and with a resolution of $2\ \text{cm}^{-1}$. Each resulting spectrum was derived from the co-addition of 20 scans under these conditions. Authentic samples of reactants and products were used to calibrate reference spectra.

Absolute Rate Studies. Absolute rate studies were carried out with the technique of pulsed laser photolysis−laser induced fluorescence (PLP-LIF). The experimental setup used in these kinetic studies has been described in detail elsewhere and only a brief summary is given here.[12] A KrF excimer laser (Lambda Physik LPX 105i) was employed to generate OH radicals by the photolysis of H_2O_2 at 248 nm.

$$H_2O_2 + h\nu\ (\lambda = 248\ \text{nm}) \rightarrow OH + OH \qquad (5)$$

The energy of the photolysis laser was of the order 2 to 15 mJ per pulse in the cell and the duration of the pulse was equal to 23 ns, full width at half-maximum (fwhm). A Nd:YAG (Continuum) pumped frequency-doubled dye laser, which was triggered at a variable time after the photolysis pulse, was used to determine the concentrations of hydroxyl radicals by laser induced fluorescence (LIF). The duration of this probe pulse was equal to 7 ns, full width at half-maximum (fwhm). The probe operated to excite the Q_11, Q_11^1, and R_23 lines in the (1,0) of the $(A^2\Sigma^+, v' = 1) \leftarrow (X^2\Pi, v'' = 0)$ transition of the OH radical at around 282 nm. The resulting fluorescence of the hydroxyl radical was collected by a photomultiplier (PM) tube (Hamamatsu R292) equipped with band-pass filter (309.4 nm peak transmission, fwhm = 7.6 nm). Hydrogen peroxide (70 wt % in water) was concentrated by bubbling helium through the solution for several days prior to use to remove water. It was admitted into the reaction cell by passing a small flow of helium through a glass bubbler containing H_2O_2. The reaction mixture, consisting of measured amounts of the reactant, radical precursor (H_2O_2, $0.5-1.0 \times 10^{14}$ molecule cm^{-3}), and the bath gas (approximately 100 Torr of helium), was flowed vertically through the cell, with a linear velocity in the range of 5 to 20 cm s^{-1}, so that each photolysis/probe sequence investigated a fresh mixture and reaction products did not build up in the cell. The concentrations of reactants and the bath gas were calculated from their mass flow rates, the temperature, and the pressure in the cell. Calibrated mass flow meters and a capacitance manometer positioned adjacent to the entrance of the cell were employed to measure all flow rates and the pressure within the reaction cell, respectively. Each datum point was obtained by averaging the signals from 100 probe laser shots. An OH concentration versus time profile was obtained by averaging signals for delay times from about 10 μs to 30 ms.

Product Studies. Product studies were carried out on the OH and Cl initiated oxidation of $CF_3CH_2CH_2OH$ and CF_3CH_2CHO both in the absence and presence of NO_x under laboratory conditions and at the European Photoreactor (EUPHORE) outdoor facility in Valencia, Spain. An experimental protocol similar to that described in the relative rate Experimental Section was used in laboratory product studies. Hydroxyl radicals in the product distribution studies were generated by the photolysis of H_2O_2 at 254 nm and analyses of reaction mixtures was by FTIR spectroscopy.

The reaction chamber employed for product studies at the EUPHORE facility consisted of a half-spherical FEP Teflon chamber with a volume of around 195 000 L mounted on aluminum floor panels covered with FEP Teflon foil. The FEP Teflon had a transmission of more than 80% over the wavelength range 280 to 640 nm. A hydraulically operated steel housing surrounded the chamber and allowed the exposure time to sunlight to be controlled. Heating of the reaction mixtures above ambient temperature was compensated with cooling by a refrigeration system housed in the chamber floor. Typically, the chamber temperature was in the range 300 ± 5 K. The chamber was filled with air from the air purification system consisting of absorption dryers connected to charcoal scrubbers. Two mixing fans housed in the chamber were used to ensure homogeneous reaction mixtures. Measured volumes of gaseous and liquid samples were introduced into the covered reaction chamber through Teflon tubing by a stream of purified air. Hydroxyl radicals and Cl atoms were generated by the solar photolysis of HONO and ClC(O)C(O)Cl, respectively.

$$HONO + h\nu\ (\lambda > 300\ \text{nm}) \rightarrow OH + NO \qquad (6)$$

$$ClC(O)C(O)Cl + h\nu\ (\lambda > 300\ \text{nm}) \rightarrow 2Cl + 2CO \qquad (7a)$$

$$\rightarrow CCl_2O + CO \qquad (7b)$$

HONO was continuously added to the chamber during the photolysis to maintain the concentration in the range 10−20 ppm. Losses of reactants and products occurred by leakage from the chamber, which was maintained at several Torr above ambient pressure. The leak rate was determined by adding an unreactive tracer gas, SF_6, to the chamber. The loss of reactants and formation of products was monitored with a Nicolet Magna 550 FTIR spectrometer equipped with an MCT detector. Infrared spectra were obtained by in situ long-path absorption, and were derived from the co-addition of 128 scans recorded by using a path length of 326.8 m over the range 400−4000 cm^{-1} with a resolution of 1 cm^{-1}. The reactants and products were quantified by using calibrated reference spectra.

Materials

Synthetic air, zero-grade (Air Products), helium carrier gas (UHP certified to >99.9995%, Alpha gas), H_2O_2 (70 wt % in water, Interox Chemie), Cl_2 99.95% (Aldrich), ClC(O)C(O)Cl 99% (Aldrich), SF_6 99.75+% (Aldrich), $CF_3CH_2CH_2OH$ 97% (Fluorochem), $C_6F_{13}CH_2CH_2OH$ 97% (Atofina company) CF_3CH_2CHO 97% (Fluorochem), n-C_6H_{14} 99% (Aldrich), HC(O)-OC_2H_5 97% (Aldrich), CFH_2CH_2OH 95% (Aldrich), and $HC(O)O(CH_2)_3CH_3$ 97% (Aldrich) were used. Samples of the compounds were stored in evacuated glass vessels and subjected to freeze−pump−thaw cycles prior to use. Trifluoroacetaldehyde was prepared by the addition of 1-ethoxy-2,2,2-trifluoroethanol 90% (Aldrich) to concentrated sulfuric acid 99.99+% (Aldrich), distilled off under vacuum and trapped at liquid nitrogen temperature. The purity of the product was estimated by IR spectroscopy to be better than 98%. Photolysis of CF_3I 99% (Fluorochem) at $\lambda > 300$ nm in air was used to generate CF_2O. Nitrous acid was generated from the reaction of sodium nitrite 99.99+% (Aldrich) with sulfuric acid 99.99+% (Aldrich).

Results

Relative Rate Studies. Relative rate coefficients for the reaction of OH radicals and chlorine atoms with $CF_3CH_2CH_2OH$ and CF_3CH_2CHO, and for the reaction of OH radicals with $C_6F_{13}CH_2CH_2OH$ were determined by comparing their rates of decay with reference compounds whose rate constants have been previously established. In the presence of OH radicals or atomic chlorine the substrate and reference compounds decay due to reactions 8 and 9.

$$\text{OH/Cl} + \text{substrate} \rightarrow \text{products} \quad (8)$$

$$\text{OH/Cl} + \text{reference} \rightarrow \text{products} \quad (9)$$

Provided that both substrate and reference are only lost by reaction with OH radicals, or Cl atoms, neither organic is reformed in any process, and the dilution due to sampling is negligible it can be shown that

$$\ln\{[\text{substrate}]_0/[\text{substrate}]_t\} = k_8/k_9 \ln\{[\text{reference}]_0/[\text{reference}]_t\} \quad (I)$$

where the subscripts 0 and t indicate concentrations at the start of the reaction and at time t, respectively. 3,3,3-Trifluoropropanol, tridecafluorooctanol, 3,3,3-trifluoropropanal, and the reference compounds employed were shown to be stable in the dark and photolytic loss of reactants and reaction products was found to be negligible over the time period of the kinetic experiments. At least three individual runs were carried out for each of the substrates with a particular reference compound. The experimental values of $[\text{substrate}]_0/[\text{substrate}]_t$ and $[\text{reference}]_0/[\text{reference}]_t$ have estimated errors of 2%. Figure 1 shows the relative rate plots for the reaction of OH radicals with $CF_3CH_2CH_2OH$, with 2-fluoroethanol, n-butyl formate, and n-hexane as reference compounds. Relative rate plots for the reaction of OH radicals with $C_6F_{13}CH_2CH_2OH$ with n-butyl formate and n-hexane as reference compounds are shown in Figure 2. The values of $[C_6F_{13}CH_2CH_2OH]_0/[C_6F_{13}CH_2CH_2OH]_t$ at low conversions of the alcohol are subject to large experimental error and the regression lines in Figure 2 are forced through the origin by using a weighted least-squares method. The relative rate data for the reactions of Cl with $CF_3CH_2CH_2OH$ or CF_3CH_2CHO, using $HC(O)OC_2H_5$ as the reference compound, are represented in Figure 3. Table 1 summarizes the measured ratios k_8/k_9, the rate coefficients for the reactions of OH and Cl with the reference compounds, and the derived values of k_8.

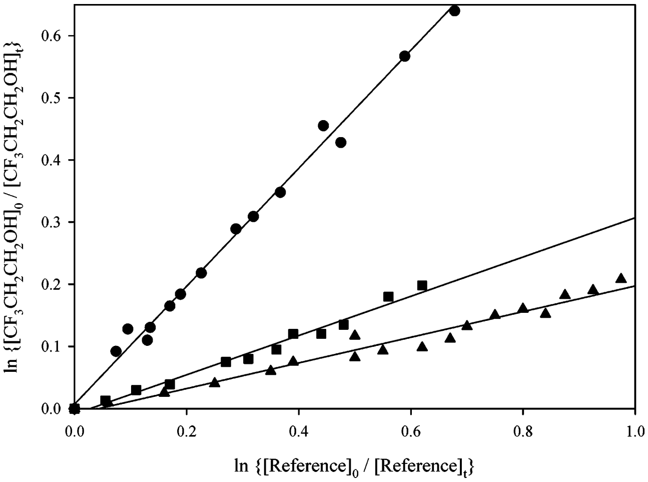

Figure 1. Concentration−time profiles for the reaction of OH radicals with $CF_3CH_2CH_2OH$ with 2-fluoroethanol (●), n-butyl formate (■), and n-hexane (▲) as reference compounds at 298 ± 2 K and atmospheric pressure.

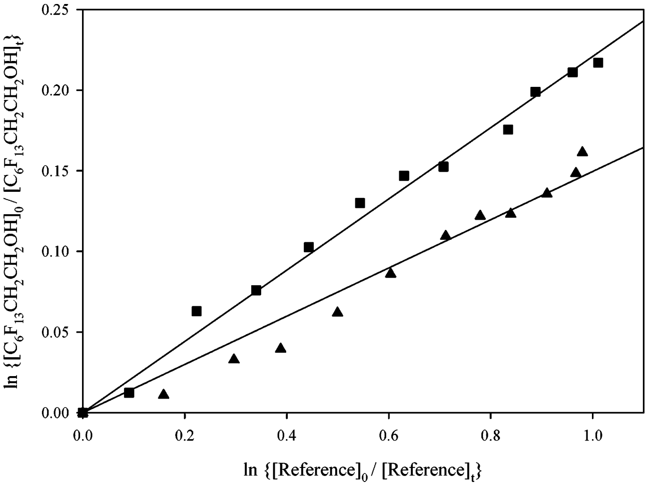

Figure 2. Concentration−time profiles for the reaction of OH radicals with $C_6F_{13}CH_2CH_2OH$ with n-butyl formate (■) and n-hexane (▲) as reference compounds at 298 ± 2 K and atmospheric pressure.

Absolute Rate Studies. All absolute rate kinetic experiments were carried out under pseudo-first-order conditions with the concentration of substrate compounds in large excess over the concentration of hydroxyl radicals, $[\text{substrate}]_0 \gg [\text{OH}]_0$.

$$H_2O_2 + h\nu\ (\lambda = 248\ \text{nm}) \rightarrow \text{OH} + \text{OH} \quad (5)$$

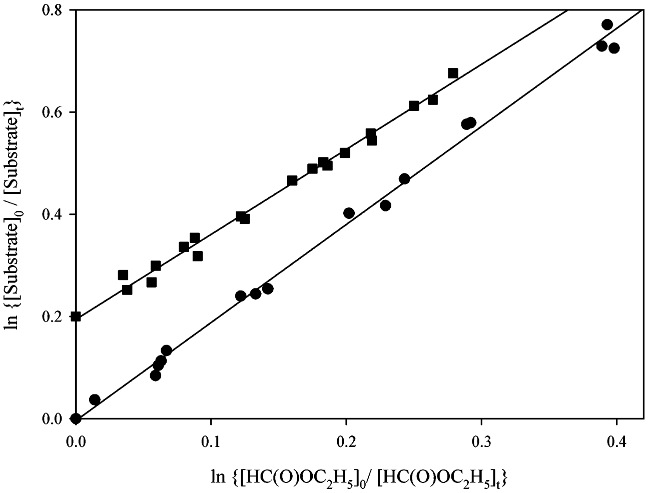

Figure 3. Concentration−time profiles for the reaction of Cl atoms with $CF_3CH_2CH_2OH$ (■) and CF_3CH_2CHO (●) with $HC(O)OC_2H_5$ as the reference compound at 298 ± 2 K and atmospheric pressure. The values of ln{[substrate]$_0$/[substrate]$_t$} in the $CF_3CH_2CH_2OH/HC(O)OC_2H_5$ system have been offset by 0.2 for clarity of presentation.

Following OH formation from photolysis of H_2O_2, reaction 5, the radical can be lost via the following processes:

$$\mathrm{OH} + \text{substrate} \rightarrow \text{products} \tag{8}$$

$$\mathrm{OH} + \mathrm{H_2O_2} \rightarrow \text{products} \tag{10}$$

$$\mathrm{OH} + \text{impurities} \rightarrow \text{products} \tag{11}$$

$$\mathrm{OH} \rightarrow \text{diffusion out of the detection zone} \tag{12}$$

hence

$$-\mathrm{d[OH]/d}t = (k_8[\text{substrate}] + k_{10}[\mathrm{H_2O_2}] + k_{11}[\text{impurities}] + k_{12})[\mathrm{OH}]$$

In the absence of perturbations due to secondary reactions, the rate of disappearance of the OH radical follows a simple exponential rate law:

$$[\mathrm{OH}]_t = [\mathrm{OH}]_0 e^{-k'_t}$$

where $k' = k_8[\text{substrate}] + k'_0$.

The rate coefficient k'_0 represents the first-order decay of OH radicals in the absence of substrate and depends on the rate of reaction of OH with H_2O_2, diffusion out of the detection zone, and the rate of reaction of hydroxyl radicals with any impurities present in the substrate. The impurities present in $CF_3CH_2CH_2OH$ and CF_3CH_2CHO after vacuum distillation were found to be traces (<1%) of $CF_3CF_2CH_2OH$ and CF_3CF_2CHO, respectively. Since the compounds have considerably lower rate coefficients for reaction with OH than the substrate compounds it can be assumed that reaction of OH radicals with impurities is negligible, therefore:

$$k'_0 = k_{10}[\mathrm{H_2O_2}] + k_{12}$$

Values for k'_0 were measured to be in the range 50−300 s^{-1}. Substrate concentrations and the measured first-order rate coefficients k' have estimated errors of 2%. Plots of k' versus the substrate concentration for the reaction of OH radicals with $CF_3CH_2CH_2OH$ and CF_3CH_2CHO exhibit excellent linearity, Figure 4. Due to the relatively low vapor pressure of $CF_3CH_2CH_2OH$, the maximum attainable experimental concentration of $CF_3CH_2CH_2OH$ was 18 × 10^{-14} molecule cm^{-3}. Absolute rate coefficients, k_8, were derived from least-squares fits of the data and are listed in Table 1.

Product Studies. Products from the OH radical and Cl atom initiated oxidations of 3,3,3-trifluoropropanol and 3,3,3-trifluoropropanal were investigated by using FTIR spectroscopy in laboratory and outdoor reaction chambers both in the absence and presence of NO_x. The initial mixing ratios of reactants in laboratory chamber studies were the following: [fluoro alcohol]$_0$ or [fluoroaldehyde]$_0$ = 40−80 ppm, $[Cl_2]_0$ = 40−120 ppm or $[H_2O_2]_0$ = 50−100 ppm, $[NO_x]_0$ = 0−20 ppm. For reactions carried out at EUPHORE the initial mixing ratios of the fluorinated compounds were in the range 0.7−1.0 ppm and the radical sources HONO and ClC(O)C(O)Cl had mixing ratios of 10−20 and 1−5 ppm, respectively. The initial product of the OH and Cl initiated oxidation of $CF_3CH_2CH_2OH$ was CF_3CH_2CHO, which decays relatively rapidly to form the secondary product CF_3CHO. For reactions carried out in the presence of NO_x, a small amount of the peroxyacyl nitrate $CF_3CH_2C(O)O_2NO_2$ was also produced as a secondary product. At longer reaction times CF_3CHO was slowly removed from the system generating CF_2O, $CF_3C(O)OH$, and $CF_3O_3CF_3$ in the absence of NO_x, and CF_2O and $CF_3C(O)O_2NO_2$ in the presence of NO_x.

Results from an experiment carried out in the outdoor simulation chamber involving the Cl atom initiated oxidation of $CF_3CH_2CH_2OH$ in the absence of NO_x are presented in Figures 5−8. Infrared spectra recorded at the start of the reaction and after 50 min of sunlight irradiation of a mixture of $CF_3CH_2CH_2OH$ (0.73 ppm) and ClC(O)C(O)Cl (1.0 ppm) in air at atmospheric pressure are shown in Figure 5. Loss of the fluoro alcohol in this experiment after 50 min is approximately 70%. Reference spectra of the fluoroaldehydes CF_3CH_2CHO, CF_3CHO, and CF_2O are given in Figure 6. Concentration−time profiles of reactants and products and product yield plots are shown in Figures 7 and 8, respectively. Figure 9 shows the concentration−time profiles of the reactants and products from an experiment performed under laboratory conditions in which a mixture of $CF_3CH_2CH_2OH$ (54 ppm) and H_2O_2 (100 ppm) was photolyzed in the absence of NO_x until around 50% of the $CF_3CH_2CH_2OH$ had been lost. The product yield plot is given in Figure 10. The OH radical and Cl atom initiated oxidation of CF_3CH_2CHO was also investigated under laboratory conditions and in the outdoor simulation chamber. In the absence of NO_x, CF_3CHO was formed in almost quantitative yields, whereas in experiments conducted in the presence of NO_x, $CF_3CH_2C(O)O_2NO_2$ was also formed. At longer reaction times small amounts of CF_3CHO were lost from the system giving mainly CF_2O.

Discussion

Kinetic Studies. The average value of the rate coefficient for the reaction of OH with $CF_3CH_2CH_2OH$ derived from our relative rate measurements k_8(OH + $CF_3CH_2CH_2OH$) = (1.08 ± 0.05) × 10^{-12} cm^3 $molecule^{-1}$ s^{-1} is in reasonable agreement with the value of k_8(OH + $CF_3CH_2CH_2OH$) = (0.89 ± 0.03) × 10^{-12} cm^3 $molecule^{-1}$ s^{-1} obtained in this work by using a LP-LIF absolute rate technique. The rate coefficient for reaction of OH with CF_3CH_2CHO from LP-LIF measurements k_8(OH + CF_3CH_2CHO) = (2.96 ± 0.04) × 10^{-12} cm^3 $molecule^{-1}$ s^{-1} is also somewhat lower than the value of (3.6 ± 0.3) × 10^{-12} cm^3 $molecule^{-1}$ s^{-1} recently reported from our laboratory from relative rate studies.[17] The reasons for these small discrepancies are not clear. No data have previously been reported for the reactions of OH and Cl with $CF_3CH_2CH_2OH$ and CF_3CH_2CHO.

TABLE 1: Rate Data for the Reaction of OH Radicals and Cl Atoms with $CF_3CH_2CH_2OH$ and CF_3CH_2CHO and for the Reaction of OH with $C_6F_{13}CH_2CH_2OH$ at 298 ± 2 K

substrate	reference	$k_8/k_9{}^{a}$	$10^{12}k_9{}^{a,b}$	$10^{12}k_8{}^{b,c}$ relative rate	$10^{12}k_8{}^{a,b}$ absolute rate
		OH kinetics			
$CF_3CH_2CH_2OH$	$HC(O)O(CH_2)_3CH_3$	0.30 ± 0.01	3.54 ± 0.52^{d}	1.06 ± 0.04	0.89 ± 0.03
	$CH_3(CH_2)_4CH_3$	0.20 ± 0.01	5.45 ± 0.16^{e}	1.09 ± 0.05	
	CFH_2CH_2OH	0.95 ± 0.02	1.15 ± 0.02^{f}	1.09 ± 0.02	
$C_6F_{13}CH_2CH_2OH$	$HC(O)O(CH_2)_3CH_3$	0.22 ± 0.01	3.54 ± 0.52^{d}	0.76 ± 0.05	
	$CH_3(CH_2)_4CH_3$	0.15± 0.01	5.45 ± 0.16^{e}	0.82 ± 0.10	
CF_3CH_2CHO					2.96 ± 0.04
		Cl kinetics			
$CF_3CH_2CH_2OH$	$HC(O)OC_2H_5$	1.67 ± 0.03	13.4 ± 0.15 ^{g}	22.4 ± 0.4	
CF_3CH_2CHO	$HC(O)OC_2H_5$	1.92 ± 0.03	13.4 ± 0.15^{g}	25.7 ± 0.4	

[a] Errors are twice the standard deviation and represent precision only. [b] In units of cm^3 molecule^{-1} s^{-1}. [c] Errors are twice the standard deviation and represent precision only: errors in the reference rate coefficients are not included in the derived values of k_8 but will probably add a further 15% to the error in the reported rate constant. [d] Le Calvé et al.[13] [e] Donahue et al.[14] [f] Kelly et al.[15] [g] Notario et al.[16]

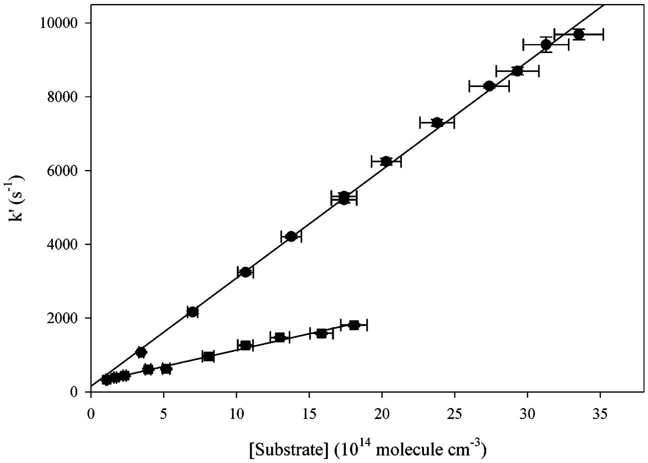

Figure 4. Plots of k' for the reaction of OH radicals with CF_3CH_2CHO and $CF_3CH_2CH_2OH$ versus the concentrations of CF_3CH_2CHO (●) and $CF_3CH_2CH_2OH$ (■) at 298 K.

For the reaction of OH with $C_6F_{13}CH_2CH_2OH$ our rate constant value, $k_8(OH + C_6F_{13}CH_2CH_2OH) = (0.79 \pm 0.08) \times 10^{-12}$ cm^3 molecule^{-1} s^{-1}, agrees within the quoted errors with those of Ellis et al.,[4] who have recently measured the rate coefficients for reaction of OH with a series of fluorotelomer alcohols of structure $F(CF_2CF_2)_nCH_2CH_2OH$ ($n = 2, 3, 4$), using a relative rate method. They reported a rate coefficient of $k(OH + F(CF_2CF_2)_nCH_2CH_2OH) = (1.07 \pm 0.22) \times 10^{-12}$ cm^3 molecule^{-1} s^{-1}. Our value and that of Ellis et al.[4] are similar to that determined in this study for reaction of OH with 3,3,3-trifluoropropanol. Thus, as might be expected, substitution of the methyl group in propanol by any totally fluorinated alkyl group results in essentially the same change in reactivity of propanol with respect to reaction with the OH radical.

Kinetic and mechanistic data for the reaction of OH[18,19] and Cl[20] with aliphatic alcohols show that hydrogen atom abstraction occurs mainly from the α-carbon atom and that alcohols are considerably more reactive than the corresponding alkanes. Thus, abstraction from the $-CH_2-$ group in ethanol by OH is around three times more facile than abstraction from a $-CH_2-$ group in alkanes. These results can be rationalized largely in terms of the reduction in the carbon−hydrogen bond strength at the α-position in alcohols: $D(CH_3CHOH{-}H) = 389$ kJ mol^{-1} and $D(CH_3CHCH_3{-}H) = 409$ kJ mol^{-1}.[21] It is apparent from the reported rate data for OH and Cl that fluorine substitution in alkanes substantially reduces their reactivity. For example, the rate coefficient for reaction of OH with CF_3CH_3 is over 2 orders of magnitude lower than that for reaction with ethane.[21]

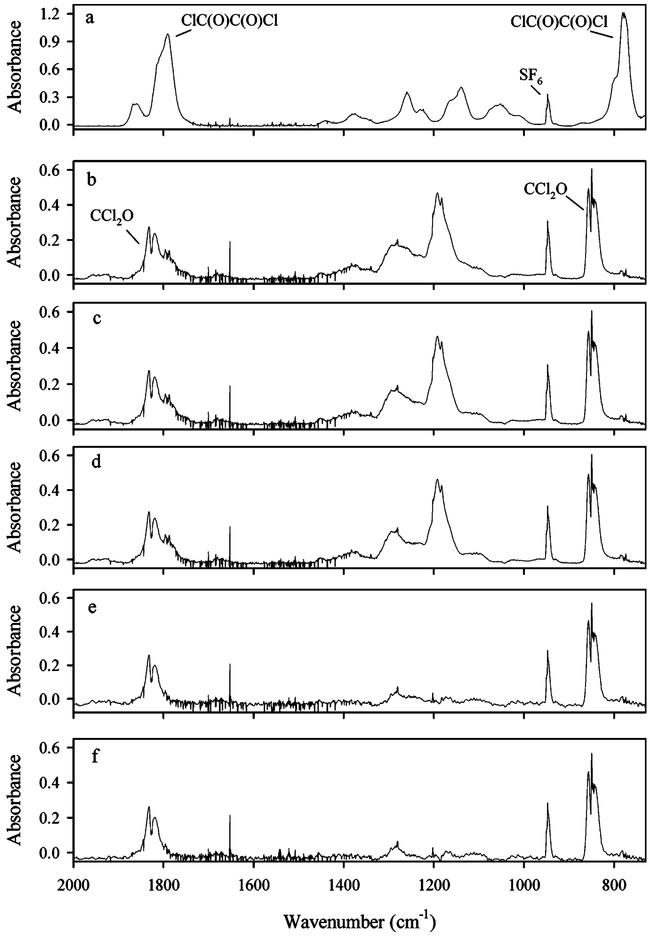

Figure 5. IR spectra from the Cl atom initiated oxidation of $CF_3CH_2CH_2OH$ carried out at EUPHORE in the absence of NO_x (a) before photolysis, (b) after 50 min of photolysis, and after successive subtractions of (c) $CF_3CH_2CH_2OH$, (d) CF_3CH_2CHO, (e) CF_3CHO, and (f) CF_2O.

Fluorine substitution at the β-carbon atom in alkanes causes only a relatively small increase in the bond dissociation energy at the α-carbon atom: $D(CF_3CH_2{-}H) = 447$ kJ mol^{-1} and $D(CH_3CH_2{-}H) = 423$ kJ mol^{-1}.[21] Hence, it seems unlikely that the increase in the C−H bond strength in CF_3CH_3 is the major factor in the large reduction in reactivity and suggests that the inductive electron withdrawing effect of the $-CF_3$ group destabilizes the transition state for the reaction. The rate coefficients for the reactions of OH[6,7,10,15] and Cl[9,10,15] with trifluoroethanol are approximately 30 and 150 times, respec-

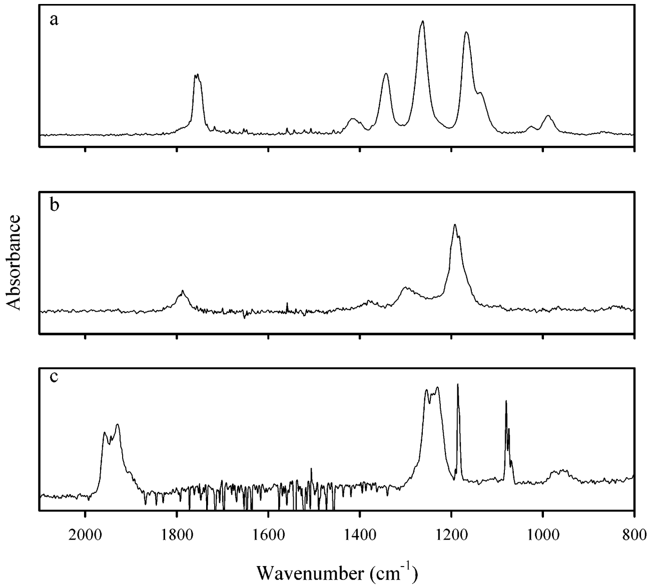

Figure 6. IR spectra of (a) CF_3CH_2CHO, (b) CF_3CHO, and (c) CF_2O.

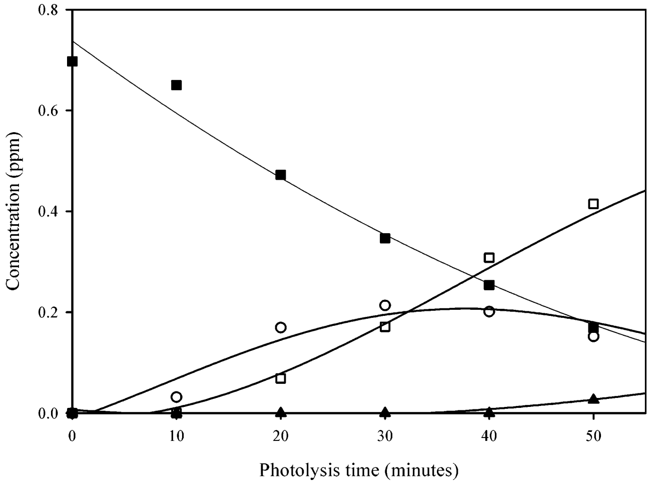

Figure 7. Concentration–time profiles of reactants and products from the reaction of Cl atoms with $CF_3CH_2CH_2OH$ in the absence of NO_x at EUPHORE at 300 ± 5 K: $CF_3CH_2CH_2OH$ (■), CF_3CH_2CHO (○), CF_3CHO (□), and CF_2O (▲).

tively, lower than those for the corresponding strongly exothermic reactions with ethanol. Bond dissociation energies have not been determined for fluorinated alcohols; however, recent quantum mechanical calculations indicate that the C–H bond strength at the α-position in CF_3CH_2OH is less than 10 kJ mol^{-1} higher than that in ethanol.[9] Therefore, it seems reasonable to assume that fluorination will not sufficiently strengthen the $CF_3CHOH-H$ bond to account for the observed reactivity trends. It is proposed that the relatively large changes in reactivity are mainly due to inductive effects in the transition states. The transition states of highly exothermic reactions are normally assumed to be similar in structure and energy to those of the reactants. Hence, the considerable charge separation in CF_3CH_2OH will be reflected in the loose transition states formed in reactions with OH and Cl. The transition states involve a hydrogen atom positioned between the electrolphilic OH or Cl species and the CF_3CHOH radical. Fluorine substitution of the hydrogen atoms in the $-CH_3$ group in ethanol will reduce the electron density on the H atom abstracted from the α-CH_2– group and thus destabilize the transition state compared to that formed with CH_3CH_2OH. In a similar manner, the rate coefficients for the reaction of OH[17,22,23] and Cl[22,24] with CF_3CHO are very much lower than those for reaction with CH_3CHO. These results have also been explained mainly in terms of destabilization of the transition states for reaction by the electron withdrawing inductive effect of the $-CF_3$ group rather than by an increase in the $CF_3C(O)-H$ bond energy.[22]

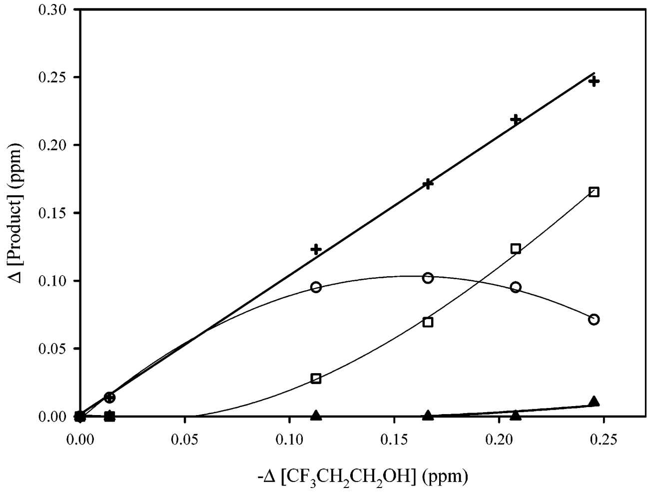

Figure 8. Product yield plots for the reaction of Cl atoms with $CF_3CH_2CH_2OH$ in the absence of NO_x at EUPHORE at 300 ± 5 K: CF_3CH_2CHO (○), CF_3CHO (□), CF_2O (▲), and total product yield (+).

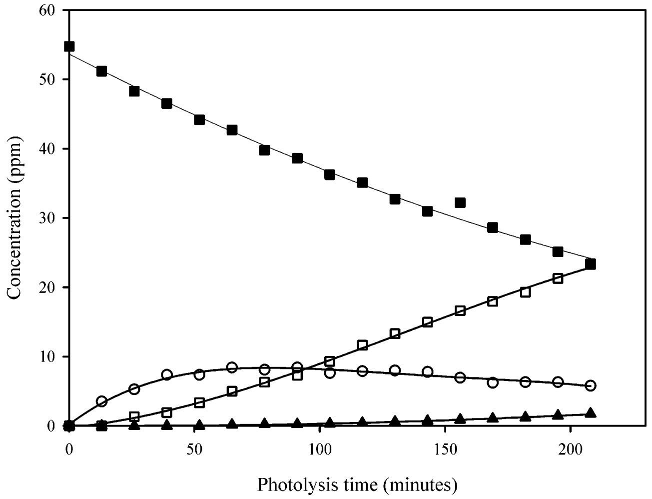

Figure 9. Concentration–time profiles of reactant and products from the reaction of OH radicals with $CF_3CH_2CH_2OH$ in the absence of NO_x under laboratory conditions at 298 ± 2 K: $CF_3CH_2CH_2OH$ (■), CF_3CH_2CHO (○), CF_3CHO (□), and CF_2O (▲).

The rate coefficients for the reactions of OH and Cl with $CF_3CH_2CH_2OH$ determined in the present work are about five times smaller than those for the corresponding reactions with *n*-propanol. Hydrogen atom abstraction is expected to take place almost exclusively at the α-CH_2– group since the presence of the $-CF_3$ group will strongly deactivate the β-position. Product studies in this study support this conclusion. The reaction of OH with $C_6F_{13}CH_2CH_2OH$ will proceed through a similar primary mechanism since the rate constant of this reaction is almost the same as that of reaction of OH with $CF_3CH_2CH_2OH$. A similar decrease in the reactivity of CF_3CH_2CHO in reactions with OH and Cl is observed compared to their reactivity with CH_3CH_2CHO. Since the C–H bond strengths at the α-CH_2– group in $CF_3CH_2CH_2OH$ and at the aldehydic group in CF_3CH_2CHO are expected to be similar to those in $CH_3CH_2CH_2OH$ and CH_3CH_2CHO, respectively, the reduction in reactivity of $CF_3CH_2CH_2OH$ and CF_3CH_2CHO must reflect the long-range destabilizing inductive effect of the $-CF_3$ group

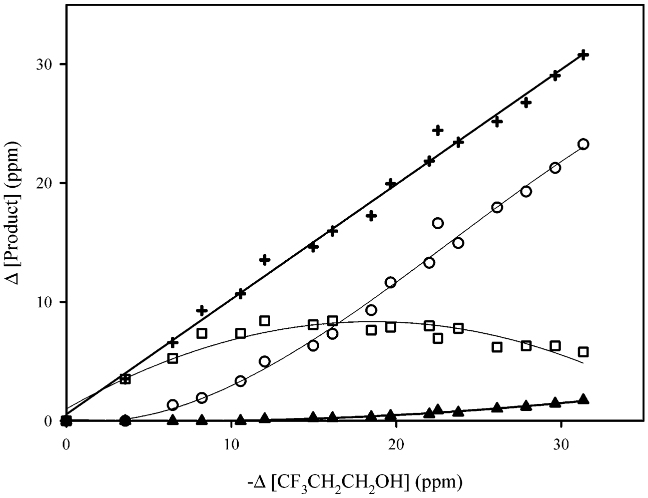

Figure 10. Product yield plots for the reaction of OH radicals with $CF_3CH_2CH_2OH$ in the absence of NO_x under laboratory conditions at 298 ± 2 K: CF_3CH_2CHO (○), CF_3CHO (□), CF_2O (▲), and total product yield (+).

in the transition states for the reactions. Kwok and Atkinson[25] have previously found that the rate coefficients estimated from simple structure−activity relationships, which consider only next neighbor atomic groups, result in higher values than experimentally observed when applied to reactions of OH radicals with fluorinated compounds. They pointed out that the long-range deactivating effect of fluorinated groups must be incorporated into the relationships to obtain reasonable agreement between calculated and experimental rate coefficients.

Reaction Products. The only primary product formed in both the OH and Cl initiated oxidation of 3,3,3-trifluoropropanol was 3,3,3-trifluoropropanal and production of the aldehyde was unaffected by the presence of NO_x in the system. This observation is consistent with hydrogen atom abstraction from the α-CH_2− group in $CF_3CH_2CH_2OH$. Abstraction of a hydrogen atom from the β position in $CF_3CH_2CH_2OH$ would lead to the generation of the $CF_3CH(O)CH_2OH$ radical. This species would give rise to CF_3CHO by C−C bond fission. The absence of CF_3CHO as an initial product from both the OH and Cl initiated oxidation reactions suggests that abstraction from the β-CH_2− group is negligible. The α-hydroxy alkyl radical, produced by abstraction of a hydrogen atom from the α-CH_2− group, reacts directly with molecular oxygen to give the aldehyde.

$$\mathrm{OH/(Cl)} + \mathrm{CF_3CH_2CH_2OH} \rightarrow \mathrm{H_2O/(HCl)} + \mathrm{CF_3CH_2CHOH} \quad (13)$$

$$\mathrm{CF_3CH_2CHOH} + \mathrm{O_2} \rightarrow \mathrm{CF_3CH_2CHO} + \mathrm{HO_2} \quad (14)$$

3,3,3-Trifluoropropanal was fairly rapidly removed from the system following abstraction of the aldehydic H atom by reaction with OH or Cl.

$$\mathrm{OH/(Cl)} + \mathrm{CF_3CH_2CHO} \rightarrow \mathrm{H_2O/(HCl)} + \mathrm{CF_3CH_2C(O)} \quad (15)$$

The concentration−time profiles of $CF_3CH_2CH_2OH$ and the primary oxidation product CF_3CH_2CHO are a function of the relative values of the rate coefficients for the reactions of OH or Cl with these compounds. Rate data from this work gives the following: $k_{13}(\mathrm{OH} + \mathrm{CF_3CH_2CH_2OH})/k_{15}(\mathrm{OH} + \mathrm{CF_3CH_2CHO}) = 0.3$ and $k_{13}(\mathrm{Cl} + \mathrm{CF_3CH_2CH_2OH})/k_{15}(\mathrm{Cl} + \mathrm{CF_3CH_2CHO}) = 0.9$. Hence for reaction with OH the aldehyde is considerably more reactive than the initial reactant, while for the reaction with Cl both compounds have virtually the same degree of reactivity. Thus, as is demonstrated in Figures 7 and 9 the maximum yield of primary product CF_3CH_2CHO is significantly lower for reaction with OH than that observed for reaction with Cl. As a consequence, formation of the major secondary product CF_3CHO occurs much more rapidly when the oxidation is initiated by OH radicals.

Degradation of CF_3CH_2CHO gives CF_3CHO as the major product. The combined yields of CF_3CH_2CHO and CF_3CHO were (0.95 ± 0.05) for OH and Cl initiated oxidations carried out in the absence of NO_x in both laboratory and outdoor simulation chamber experiments for conversions of $CF_3CH_2CH_2OH$ <50%. When reactions were carried out in the presence of NO_x the combined yields of CF_3CH_2CHO and CF_3CHO were 0.80 ± 0.10. Spectral evidence indicates that small unquantified amounts of $CF_3CH_2C(O)O_2NO_2$ were also produced in these reactions. In the absence of NO_x the product distribution yields can be rationalized in terms of the following reaction scheme:

$$\mathrm{CF_3CH_2C(O)} + \mathrm{O_2} + \mathrm{M} \rightarrow \mathrm{CF_3CH_2C(O)O_2} + \mathrm{M} \quad (16)$$

$$\mathrm{CF_3CH_2C(O)O_2} + \mathrm{RO_2} \rightarrow \mathrm{CF_3CH_2C(O)O} + \mathrm{RO} + \mathrm{O_2} \quad (17)$$

$$\mathrm{CF_3CH_2C(O)O} \rightarrow \mathrm{CO_2} + \mathrm{CF_3CH_2} \quad (18)$$

$$\mathrm{CF_3CH_2} + \mathrm{O_2} + \mathrm{M} \rightarrow \mathrm{CF_3CH_2O_2} + \mathrm{M} \quad (19)$$

$$\mathrm{CF_3CH_2O_2} + \mathrm{RO_2} \rightarrow \mathrm{CF_3CH_2O} + \mathrm{RO} + \mathrm{O_2} \quad (20)$$

$$\mathrm{CF_3CH_2O} + \mathrm{O_2} \rightarrow \mathrm{CF_3CHO} + \mathrm{HO_2} \quad (21)$$

where RO_2 is a peroxy radical.

Reaction of the acyl peroxy radical, $CF_3CH_2C(O)O_2$, with HO_2 may give rise to the formation of the corresponding acid and peracid.

$$\mathrm{CF_3CH_2C(O)O_2} + \mathrm{HO_2} \rightarrow \mathrm{CF_3CH_2C(O)OH} + \mathrm{O_3} \quad (22)$$

$$\rightarrow \mathrm{CF_3CH_2C(O)OOH} + \mathrm{O_2} \quad (23)$$

$$\rightarrow \mathrm{CF_3CH_2C(O)O} + \mathrm{OH} + \mathrm{O_2} \quad (24)$$

The reactions of $CF_3C(O)O_2$ and $C_2F_5C(O)O_2$ with HO_2 have been shown to produce the corresponding carboxylic acids and alkoxy radicals with yields of around 25% and 75%, repectively.[26,27] However, $CH_3C(O)OOH$ is the major product from the reaction of $CH_3C(O)O_2$ with HO_2 while the yield of acetic acid represents only 20% of the reaction.[28] Formation of alkoxy radicals in the $CH_3C(O)O_2$ + HO_2 system appears to be negligible. No evidence for features attributable to $CF_3CH_2C(O)OH$ and $CF_3CH_2C(O)OOH$ were found in the IR spectra of the products arising from the OH and Cl initiated oxidation of $CF_3CH_2CH_2OH$ in the absence of NO_x. This observation indicates that the yields of these acids are less than 10% under the present experimental conditions. The combined yields of CF_3CH_2CHO and CF_3CHO were close to 100% (95 ± 5%), providing support for this argument.

In the presence of NO, peroxy radicals are converted to the corresponding alkoxy radicals by reaction with NO:

$$\mathrm{CF_3CH_2C(O)O_2} + \mathrm{NO} \rightarrow \mathrm{NO_2} + \mathrm{CF_3CH_2C(O)O} \quad (25)$$

and

$$CF_3CH_2O_2 + NO \rightarrow NO_2 + CF_3CH_2O \tag{26}$$

NO_2 is generated in reactions 25 and 26 and may react with the acyl peroxy radicals to give the peroxynitrate $CF_3CH_2C(O)O_2NO_2$.

$$CF_3CH_2C(O)O_2 + NO_2 + M \rightarrow CF_3CH_2C(O)O_2NO_2 + M \tag{27}$$

The rate coefficients for reaction of OH[17,22,23] and Cl[22,24] with CF_3CHO are considerably lower than those for the corresponding reactions with CF_3CH_2CHO. Hence, loss of CF_3CHO from the $CF_3CH_2CH_2OH$ oxidation systems is quite slow, Figures 6 and 8, and only occurs at high conversions of the initial reactant. The main degradation product from the oxidation of CF_3CHO is CF_2O. In the absence of NO_x small amounts of $CF_3C(O)OH$ and the trioxide were also observed, while in the presence of NO_x traces of the peroxynitrate $CF_3C(O)ONO_2$ were detected.

$$HO/(Cl) + CF_3CHO\ O_2 \xrightarrow[O_2]{} H_2O/(HCl) + CF_3C(O)O_2 \tag{28}$$

$$CF_3C(O)O_2 + RO_2 \rightarrow CF_3C(O)O + RO + O_2 \tag{29}$$

$$CF_3C(O)O_2 + HO_2 \rightarrow CF_3C(O)OH + O_3 \tag{30}$$

$$CF_3C(O)O_2 + HO_2 \rightarrow CF_3C(O)O + OH + O_2 \tag{31}$$

$$CF_3C(O)O \rightarrow CO_2 + CF_3 \tag{32}$$

$$CF_3 + O_2 + M \rightarrow CF_3O_2 + M \tag{33}$$

$$CF_3O_2 + RO_2 \rightarrow CF_3O + RO + O_2 \tag{34}$$

$$CF_3O + CF_3O_2 \rightarrow CF_3O_3CF_3 \tag{35}$$

In the OH radical experiments CF_3O radicals may react with $CF_3CH_2CH_2OH$, H_2O_2, or H_2O to give CF_3OH, which will produce CF_2O following decomposition of the alcohol.

$$CF_3O + CF_3CH_2CH_2OH/H_2O_2/H_2O \rightarrow CF_3OH + CF_3CH_2CHOH/HO_2/OH \tag{36}$$

$$CF_3OH \rightarrow CF_2O + HF \tag{37}$$

CF_2O is also probably formed in the chlorine atom initiated oxidations by reaction of CF_3O with $CF_3CH_2CH_2OH$ and degradation of CF_3OH, reactions 36 and 37. It is also possible that in this system reaction of Cl atoms with CF_3O can lead directly to CF_2O.

$$CF_3OH + Cl \rightarrow CF_2O + ClF \tag{38}$$

Oxidation in NO_x containing systems results in the conversion of peroxy to alkoxy radicals via reaction with NO and leads directly to CF_2O formation with small amounts of $CF_3C(O)O_2NO_2$ being generated.

$$CF_3C(O)O_2 + NO \rightarrow NO_2 + CF_3C(O)O \tag{39}$$

$$CF_3O_2 + NO \rightarrow NO_2 + CF_3O \tag{40}$$

$$CF_3O + NO \rightarrow CF_2O + FNO \tag{41}$$

$$CF_3C(O)O_2 + NO_2 + M \rightarrow CF_3C(O)O_2NO_2 + M \tag{42}$$

A number of experiments were carried out on the direct OH and Cl initiated oxidation of the primary product, CF_3CH_2CHO generated in the $CF_3CH_2CH_2OH$ system. As expected, the major product is CF_3CHO formed with a yield close to unity. At high conversions, the degradation of CF_3CHO leads to CF_2O production as previously outlined.

Atmospheric Consequences

The atmospheric removal of $CF_3CH_2CH_2OH$ will be initiated by reaction with OH radicals. Photolysis is unimportant since it does not absorb radiation at actinic wavelengths. Using the averaged rate coefficient $k(OH + CF_3CH_2CH_2OH) = 1.03 \times 10^{-12}$ cm^3 molecule^{-1} s^{-1} obtained in this work and a global averaged OH concentration of 10^6 radicals cm^{-3} [29] yields an estimated atmospheric lifetime for $CF_3CH_2CH_2OH$ of around 12 days. The primary oxidation product of $CF_3CH_2CH_2OH$, CF_3CH_2CHO, may be lost by either reaction with OH or photolysis. The lifetime with respect to reaction with OH radicals is estimated from the rate data obtained in this study to be close to 4 days, while the photolysis lifetime has recently been reported as longer than 15 days.[17] Thus, the main degradation pathway for CF_3CH_2CHO would appear to be reaction with OH generating CF_3CHO as the major oxidation product. Oxidation of CF_3CH_2CHO in moderately polluted atmospheres containing NO_x would also be expected to form small amounts of $CF_3CH_2C(O)O_2NO_2$. Since peroxynitrates are thermally unstable with lifetimes of a few hours,[30] they can only provide a temporary reservoir for the $CF_3CH_2C(O)-$ group. Under low NO_x conditions, reaction of the $CF_3CH_2C(O)O_2$ radical with HO_2 could lead to the formation of the corresponding carboxylic acid.[27] The potential importance of the reaction of $CF_3CH_2C(O)O_2$ with HO_2 as a source of $CF_3CH_2C(O)OH$ is dependent on the rate coefficients for the reaction of $CF_3CH_2C(O)O_2$ with NO and HO_2 and their atmospheric concentrations.

It is evident that the major atmospheric oxidation product of $CF_3CH_2CH_2OH$ will be trifluoroacetaldehyde. The atmospheric lifetime of CF_3CHO has been estimated from the available OH rate coefficients[17,22,23] and photolysis data[17] as approximately 25 days and greater than 27 days for reaction with OH and photolysis, respectively. Reaction of OH with CF_3CHO produces the $CF_3C(O)O_2$ radical, which in the presence of NO_x generates CF_2O and the unstable compound $CF_3C(O)O_2NO_2$. As outlined above for $CF_3CH_2C(O)O_2$, at low NO_x levels reaction of $CF_3C(O)O_2$ with HO_2 can provide a source of trifluoroacetic acid. Photolysis of CF_3CHO is likely to produce CF_3 radicals, which again lead to CF_2O formation. Trifluoroacetaldehyde is highly soluble in water and general circulation model calculations indicate that rainout lifetimes of such compounds depend mainly on their mode of input into the troposphere. When a species is formed fairly uniformly in the troposphere, which is the case for CF_3CHO, the average lifetime is of the order of 15−20 days.[31] Following incorporation into cloud droplets trifluoroacetaldehyde will rapidly hydrate to form $CF_3CH(OH)_2$ and in aqueous media further oxidation produces trifluoroacetic acid. If the acid is not produced prior to evaporation of the cloud droplet, gaseous $CF_3CH(OH)_2$ will be generated. Photolysis of this dialcohol is negligible and reaction with OH will be expected to yield $CF_3C(O)OH$.

$$OH + CF_3CH(OH)_2 \rightarrow H_2O + CF_3C(OH)_2 \tag{43}$$

$$CF_3C(OH)_2 + O_2 \rightarrow CF_3C(O)OH + HO_2 \tag{44}$$

Since the lifetimes of CF_3CHO with respect to loss by reaction with OH or photolysis are relatively long, uptake in surface and rainwater or cloud droplets may be an important sink for CF_3CHO and hence a source of $CF_3C(O)OH$. For long-chain fluorotelomer alcohols the data from this work and from Ellis et al.[4] indicate that the OH reaction will also be the major atmospheric loss process giving lifetimes of around 12 days. The atmospheric degradation of these long-chain fluorotelomer alcohols produce the primary aldehydes $C_nF_{2n+1}CH_2CHO$ by a series of reactions analogous to those described for $CF_3CH_2CH_2OH$. These aldehydes are expected to react predominantly with OH to form $C_nF_{2n+1}CHO$ but may provide a source of $C_nF_{2n+1}CH_2C(O)OH$ by the reaction of $C_nF_{2n+1}CH_2C(O)O_2$ with HO_2. Reaction of OH with $C_nF_{2n+1}CHO$ will generate mainly perfluoroalkoxy radicals, although reaction of $C_nF_{2n+1}C(O)O_2$ with HO_2 under low NO_x conditions could yield $C_nF_{2n+1}C(O)OH$. It is expected that the major loss processes for long-chain perfluoroalkoxy radicals will be via sequential carbon−carbon bond breaking to form CF_2O. Recently Ellis et al.[5] have suggested that in the absence of NO_x the dominant loss of perfluoroalkyl peroxy radicals is likely to be reaction with other peroxy radicals to form the corresponding perfluoroalkoxy radicals; however, the molecular channel of the peroxy−peroxy radical reaction leads to formation of perfluoro alcohols. Loss of HF from these alcohols forms perfluoroacyl fluorides, which will hydrolyze in the atmosphere to form perfluorocarboxylic acids. The long-chain fluoroaldehydes are likely to be relatively insoluble in cloud droplets but will behave as surfactants and form $C_nF_{2n+1}CH(OH)_2$ at the surface of water droplets. Evaporation of the droplet followed by reaction of the gaseous hydrates may produce the acids $C_nF_{2n+1}C(O)OH$ in a manner similar to that proposed for $CF_3CH(OH)_2$. Thus, oxidation of long-chain fluorotelomer alcohols might generate fluorinated carboxylic acids in their atmospheric degradation, although an important degradation product will be CF_2O. This compound is unreactive with OH and will not photolyze under tropospheric conditions. The most probable loss process is uptake in cloud droplets followed by hydrolysis. The atmospheric lifetimes of the fluoro alcohols and their oxidation products are sufficiently short that their contribution to radiative forcing will be negligible.

Acknowledgment. Part of this work has been carried out in conjunction with the research project “Impact of Fluorinated Alcohols and Ethers on the Environment”, which is supported by the Commission of the European Communities under the Energy, Environment and Sustainable Development Programme through contract EVK2-CT-1999-00009. G.L.B. thanks Total company (Dr Jean Marie Libre) and Telomer Research Programme for also supporting part of this work.

References and Notes

(1) Molina, M. J.; Rowland, F. S. *Nature* **1974**, *249*, 810−812.

(2) Farman, J. C.; Gardiner, B. G.; Shanklin, J. D. *Nature* **1985**, *315*, 207−210.

(3) Scientific Assessment of Ozone Depletion. Global Ozone Research and Monitoring Project-Report No. 37; World Meteorological Organization: Geneva, Switzerland, 1994; Chapter 12.

(4) Ellis, D. A.; Martin, J. W.; Mabury, S. A.; Hurley, M. D.; Sulbaek Andersen, M. P.; Wallington, T. J. *Environ. Sci. Technol.* **2003**, *37*, 3816−3820.

(5) Ellis, D. A.; Martin, J. W.; De Silva, A. O.; Mabury, S. A.; Hurley, M. D.; Sulbaek Andersen, M. P.; Wallington, T. J. *Environ. Sci. Technol.* **2004**, *38*, 3316−3321.

(6) Wallington, T. J.; Dagaut, P.; Kurylo, M. J. *J. Phys. Chem.* **1988**, *92*, 5024−5028.

(7) Tokuhashi, K.; Nagai, H.; Takahashi, A.; Kaise, M.; Kondo, S.; Sekiya, A.; Takahashi, M.; Gotoh, Y.; Suga, A. *J. Phys. Chem. A* **1999**, *103*, 2664−2672.

(8) Chen, L.; Fukuda, K.; Takenaka, N.; Bandow, H.; Maeda, Y. *Int. J. Chem. Kinet.* **2000**, *32*, 73−78.

(9) Papadimitriou, V. C.; Prosmitis, A. V.; Lazarou, Y. G.; Papagiannakopoulos, P. *J. Phys. Chem. A* **2003**, *107*, 3733−3740.

(10) Hurley, M. D.; Wallington, T. J.; Sulbaek Andersen, M. P.; Ellis, D. A.; Martin, J. W.; Mabury, S. A. *J. Phys. Chem. A* **2004**, *108*, 1973−1979.

(11) Le Bras, G.; Bossoutrot, V.; Magneron I. Final Report to the Fluorotelomer Research Programme, July 2003.

(12) Mellouki, A.; Téton, S.; Laverdet, G.; Quilgars, A.; Le Bras, G. *J. Chim. Phys. Phys. Chim. Biol.* **1994**, *91*, 473−487.

(13) Le Calvé, S.; Le Bras, G.; Mellouki, A. *J. Phys. Chem. A* **1997**, *101*, 5489−5493.

(14) Donahue, N. M.; Anderson, J. G.; Demerijian, K. *J. Phys. Chem. A* **1998**, *102*, 3121−3126.

(15) Kelly, T.; Treacy, J.; Sidebottom, H.; Bossountrot, V.; Magneron I.; Mellouki, A.; Le Bras, G. Manuscript in preparation, 2004.

(16) Notario, A.; Le Bras, G.; Mellouki, A. *J. Phys. Chem. A* **1998**, *102*, 3112−3117.

(17) Sellevåg, S. R.; Kelly, T.; Sidebottom, H.; Nielsen, C. *Phys. Chem. Chem. Phys.* **2004**, *6*, 1243−1252.

(18) Atkinson, R. *J. Phys. Chem. Ref. Data, Monogr.* **1994**, 2.

(19) Atkinson, R.; Baulch, D. L.; Cox, R. A.; Hampson, R. F., Jr.; Kerr, J. A.; Rossi, M. J.; Troe, J. *J. Phys. Chem. Ref. Data* **1999**, *28*, 191−647.

(20) Taatjes, C. A.; Christensen, L. K.; Hurley, M. D.; Wallington, T. J. *J. Phys. Chem. A* **1999**, *103*, 9805−9814.

(21) Sander, S. P.; Friedl, R. R.; Golden, D. M.; Kurylo, M. J.; Huie, R. E.; Orkin, V. L.; Moortgat, G. K.; Ravishankara, A. R.; Kolb, C. E.; Molina, M. J.; Finlayson-Pitts, B. J. Chemical Kinetics and Photochemical Data for Use in Atmospheric Studies, Jet Propulsion Laboratory, California Institute of Technology, Pasadena CA, Evaluation no. 14, 2002; Publication 02-25.

(22) Scollard, D. J.; Treacy, J. J.; Sidebottom, H. W.; Balestra-Garcia, C.; Laverdet, G.; Le Bras, G.; MacLeod, H.; Téton, S. *J. Phys. Chem.* **1993**, *97*, 4683−4688.

(23) Dóbé, S.; Khachatryan, L. A.; Bérces, T. *Ber. Bunsen-Ges. Phys. Chem.* **1989**, *93*, 847−852.

(24) Wallington, T. J.; Hurley, M. D. *Int. J. Chem. Kinet.* **1993**, *25*, 819−824.

(25) Kwok, E. S. C.; Atkinson, R. *Atmos. Environ.* **1995**, *29*, 1685−1694.

(26) Hurley, M. D.; Wallington, T. J.; Sulbaek Andersen, M. P.; Ellis, D. A.; Martin, J. W.; Mabury, S. A. *J. Phys. Chem. A* **2004**, *108*, 1973−1979.

(27) Sulbaek Andersen, M. P.; Hurley, M. D.; Wallington, T. J.; Ball, J. C.; Martin, J. W.; Ellis, D. A.; Mabury, S. A. *Chem. Phys. Lett.* **2003**, *381*, 14−21.

(28) Tyndall, G. S.; Cox, R. A.; Granier, C.; Lesclaux, R.; Moortgat, G. K.; Pilling, M. J.; Ravishankara, A. R.; Wallington T. J. *J. Geophys. Res.* **2001**, 106, 12157−12182.

(29) Prinn, R. G.; Huang, J.; Weiss, R. F.; Cunnold, D. M.; Fraser, P. J.; Simmonds, P. G.; McCulloch, A.; Harth, C.; Salameh, P.; O’Doherty, S.; Wang, R. H. J.; Porter, L.; Miller, B. R. *Science* **2001**, *292*, 1882−1888.

(30) Sulbaek Andersen, M. P.; Hurley, M. D.; Wallington, T. J.; Ball, J. C.; Martin, J. W.; Ellis, D. A.; Mabury, S. A.; Nielsen, O. J. *Chem. Phys. Lett.* **2003**, *379*, 28−36.

(31) Kindler, T. P.; Chameides, W. L.; Wine, P. H.; Cunnold, D. M.; Alyea, F. N.; Franklin, J. A. *J. Geophys. Res. Atmos.* **1995**, *100*, 1235−1251.